JACS
JOURNAL OF THE AMERICAN CHEMICAL SOCIETY
Article
Cite This: J. Am. Chem. Soc. 2019, 141, 17918−17925
pubs.acs.org/JACS

Mechanistic and Kinetic Studies of the Ring Opening Metathesis Polymerization of Norbornenyl Monomers by a Grubbs Third Generation Catalyst

Michael G. Hyatt,[†] Dylan J. Walsh,[‡] Richard L. Lord,[§] José G. Andino Martinez,[†] and Damien Guironnet*[,‡]

[†]Department of Chemistry, University of Illinois Urbana−Champaign, Urbana, Illinois 61801, United States
[‡]Department of Chemical and Biomolecular Engineering, University of Illinois Urbana−Champaign, Urbana, Illinois 61801, United States
[§]Department of Chemistry, Grand Valley State University, Allendale, Michigan 49401, United States

Supporting Information

ABSTRACT: The mechanism of ring-opening metathesis polymerization (ROMP) for a set of functionalized norbornenyl monomers initiated by a Grubbs third generation precatalyst [$(H_2IMes)(pyr)_2(Cl)_2Ru{=}CHPh$] was investigated. Through a series of $^{12}C/^{13}C$ and $^{1}H/^{2}H$ kinetic isotope effect studies, the rate-determining step for the polymerization was determined to be the formation of the metallacyclobutane ring. This experimental result was further validated through DFT calculations showing that the highest energy transition state is metallacyclobutane formation. The effect of monomer stereochemistry (exo vs endo) of two types of ester substituted monomers was also investigated. Kinetic and spectroscopic evidence supporting the formation of a six-membered chelate through coordination of the proximal polymer ester to the Ru center is presented. This chelation and its impact on the rate of polymerization are shown to vary based on the monomer employed and its stereochemistry. The combination of this knowledge led to the derivation of a generic rate law describing the rate of polymerization of norbornene monomers initiated by a Grubbs third generation catalyst.

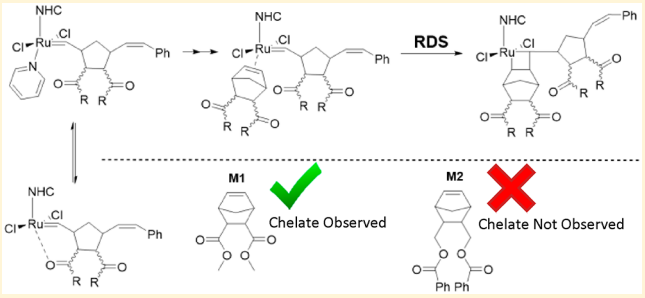

INTRODUCTION

Ring-opening metathesis polymerization (ROMP) initiated by ruthenium complexes has evolved as one of the most powerful controlled polymerization methodologies. The precision and versatility of ROMP have enabled the synthesis of sequence-controlled polymers, complex macromolecular architectures, mechanochemical responsive polymers, and self-healing polymers.[1−8] There have been many improvements to the reactivity and stability of the multiple generations of Grubbs catalysts developed over the years, with the third generation (**G3**) being the most widely employed for ROMP due to its high functional group stability, fast polymerization rates, and ability to initiate living polymerizations.[4,9−18] Since its first report, most advances in ROMP have focused primarily on the design of substrates (monomer, chain transfer agents, terminating agents), and in comparison very little work has been devoted to studying the ruthenium complex itself.[5,10,19−30] The development of **G3** was predicated on the precise knowledge of the reactivity of the second generation Grubbs catalyst (**G2**).[31,32] While the general understanding of the ROMP mechanism is extensive, the rate-determining step (RDS) of the ruthenium catalyzed polymerization of norbornenyl monomers remains unknown. In fact it was only very recently that the chemical structure of **G3** in solution, the monopyridine complex **G3-Mono**, was demonstrated to be different than the isolated solid, the dipyridine complex **G3-Di** (Chart 1).[33] Acquiring a deeper understanding of the mechanism of **G3** initiated ROMP will guide the development of new catalysts to address the remaining technical challenges, such as enhancing the reactivity of low ring-strain monomers, catalyst stability in solution, and higher endo monomer rates of polymerization.[34−36]

Chart 1. G3 Precatalyst Equilibrium Structures

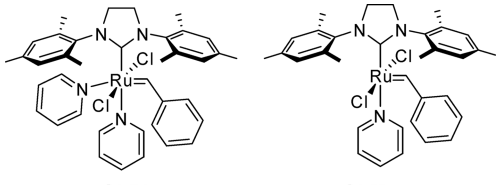

Received: September 9, 2019
Published: October 25, 2019

DOI: 10.1021/jacs.9b09752
J. Am. Chem. Soc. 2019, 141, 17918−17925

Beyond the identification of the rate-determining step, another important aspect of ROMP that is still not fully understood is the effect of stereochemistry (exo vs endo) and substituents on the rate of polymerization for norbornenyl monomers. Achieving a high rate of polymerization is advantageous for polymer synthesis, as faster rates have been shown to enable the synthesis of larger polymers with narrower molecular weight distributions, which has been particularly important for the synthesis of high density branched polymers (bottlebrush polymers).[37] Exo monomers have long been known to achieve higher rates of polymerization than their endo counterparts, thus motivating the isolation of the pure exo monomer through a tedious and wasteful process.[38,39] Beyond stereochemistry, the substituent groups/anchor groups were also found to impact the rate of polymerization, but this effect remains poorly understood due to a lack of fundamental mechanistic understanding.[5,37,40] Thus, determining the molecular features that dictate the rates of polymerization of ROMP monomers would enable the design of novel ROMP catalysts and monomers.

Herein, we report a series of kinetic isotope effect studies to identify the rate-determining step of **G3**-initiated ROMP of norbornenyl monomers. Additionally, IR experiments in conjunction with kinetic studies provide an explanation for the differences in reactivity between stereochemistries (exo and endo) of ester-containing monomers. DFT calculations are also presented to support our experimental findings and provide better insight into the interaction of the metal center and the polymer chain. The cumulative knowledge gained through this work led to the establishment of a detailed rate law for the polymerization of norbornenyl-type monomers.

RESULTS AND DISCUSSION

Rate-Determining Step. As the initiators **G2** and **G3** result in the same active species, we used the previously established reaction mechanism from **G2**-initiated ROMP for the determination of the RDS of **G3**-initiated ROMP (Scheme 1).[31,41] The first step in the mechanism is coordination of the monomer, which can occur either via an associative pathway (k_{1a}) or a dissociative pathway (k_{1b}, k_{1c}) involving a pyridine-free Ru 14-electron complex.[42] If pyridine dissociation is the RDS, then the reaction rate would be zero order in monomer.

Scheme 1. Proposed Mechanism for ROMP of Norbornene (Ligands Omitted for Clarity)

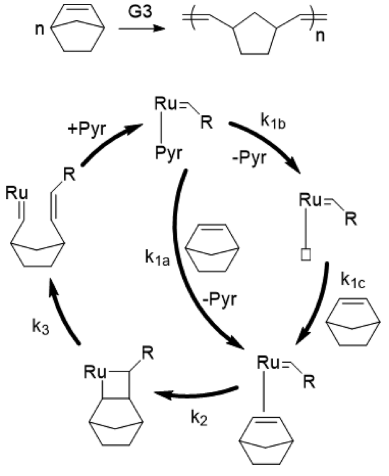

This possibility is easily discounted as **G3**-initiated ROMP is well-known to be first order in monomer.[23,33,37,40] Monomer coordination, however, could still be the RDS through an associative or dissociative pathway. We have previously demonstrated, via a series of kinetic studies, that pyridine is not coordinated to the metal during the rate determining step of the polymerization; therefore, this possibility was not considered.[33] The second step of the catalytic cycle is formation of the metallacyclobutane ring (k_2) followed by its collapse (k_3), and ultimately in coordination of pyridine. In conclusion, the RDS of ROMP can be monomer coordination, metallacyclobutane formation, or metallacyclobutane collapse. We chose to investigate the RDS of **G3**-initiated ROMP using two common norbornenyl monomers **M1** and **M2** (Chart 2) with different ester linkages (2 stereoisomers per monomer; **XX** stands for the exo monomer while **DD** stands for the endo monomer).

Chart 2. List of Monomers Used

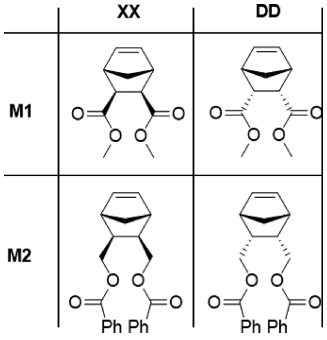

Determination of the RDS was performed through $^{12}C/^{13}C$ and $^{1}H/^{2}H$ kinetic isotope studies focusing on the olefin double bond of the monomers. The $^{12}C/^{13}C$ KIE study will indicate whether the RDS involves the breakage of a carbon−carbon bond (metallacyclobutane formation or collapse) which will have a KIE > 1, or if the RDS does not involve the breaking of a carbon−carbon bond (monomer coordination) which will have a KIE = 1. The $^{1}H/^{2}H$ KIE study will differentiate between metallacyclobutane formation and collapse. Indeed, the olefin in metallacyclobutane formation undergoes an sp^2 to sp^3 hybridization change which will have a KIE < 1, while metallacyclobutane collapse undergoes an sp^3 to sp^2 hybridization change which will have a KIE > 1. The theoretical KIE values depending on which step is rate determining are summarized in Table 1.

Table 1. Predicted KIE Values for Each Proposed RDS

Proposed RDS	$^{12}C/^{13}C$	$^{1}H/^{2}H$
monomer coordination	1	1
metallacyclobutane formation	>1	<1
metallacyclobutane collapse	>1	>1

The $^{12}C/^{13}C$ KIE was determined using the natural abundance enrichment KIE technique developed by Singleton and Thomas, as it allows for the determination of small KIEs without the need to isotopically label the starting material.[43] This technique consists of performing the reaction to high conversion and isolating the residual substrate for isotope analysis. This operation requires the use of large amounts of substrate in order to isolate sufficient quantities of unreacted

DOI: 10.1021/jacs.9b09752
J. Am. Chem. Soc. 2019, 141, 17918−17925

reagent for analysis. Using **M2-DD**, we performed a 5-g scale polymerization (18 mg **G3-Di**) to 98.5% conversion. The unreacted monomer was isolated by precipitating the polymer and was purified via preparative thin layer chromatography. As the enrichment of the ^{13}C content is expected to be small we used three independent quantification methods (^{13}C NMR, ^{1}H NMR and isotope mass spectrometry) to determine the change in the ^{13}C content. From ^{13}C NMR we measured a 3.3% enrichment in the ^{13}C content at the C=C position which corresponds to a $^{12}C/^{13}C$ KIE of 1.007_7 (± 0.001). From ^{1}H NMR, we measured a 3.5% enrichment of the ^{13}C content, by comparing the olefin peak and its ^{13}C satellites, which corresponds to a $^{12}C/^{13}C$ KIE of 1.008 (± 0.004). Then, we used isotope mass spectrometry to burn the sample and measure the relative amounts of $^{13}CO_2/^{12}CO_2$ in the combustion product to show that there is a 4.6% enrichment of the ^{13}C content at the olefin position, which corresponds to a $^{12}C/^{13}C$ KIE of 1.0109_7 ($\pm 0.0001_3$). The $^{12}C/^{13}C$ KIE data from each measurement technique agree that ROMP has a $^{12}C/^{13}C$ KIE for the olefinic carbon greater than 1, which rules out monomer coordination as the RDS. We repeated the $^{12}C/^{13}C$ KIE study with another monomer, **M1-DD**, and measured an enrichment in ^{13}C of 3.9% via ^{13}C NMR which corresponds to a $^{12}C/^{13}C$ KIE of 1.01_2 ($\pm 0.01_5$). These results suggest that the olefinic carbon−carbon bond is breaking during the rate-determining step (metallacyclobutane formation or metallacyclobutane collapse).

To differentiate between metallacyclobutane formation and metallacyclobutane collapse, we performed a $^{1}H/^{2}H$ kinetic isotope effect study. We synthesized a partially deuterated **M2-DD** that is 75% deuterated at each of the four positions indicated in Figure 1 and performed a 3-g scale polymerization

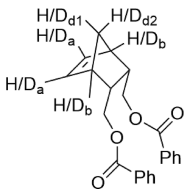

Figure 1. Partially deuterated **M2-DD**.

(11.3 mg of **G3-Di**) to 98.3% conversion. The residual monomer was isolated, purified by preparative thin layer chromatography, and analyzed by ^{1}H NMR. An enrichment in ^{1}H of 15.6% was measured at the olefinic protons which corresponds to a $^{1}H/^{2}H$ KIE of 0.965 (± 0.001). A KIE of 0.9987 (± 0.0005) was observed at the bridgehead (position b) which is consistent with there being no reaction at that position. Since the olefinic position has a $^{1}H/^{2}H$ KIE that is less than 1 and a $^{12}C/^{13}C$ KIE that is greater than 1, that means that only metallacyclobutane formation (step 2) is consistent with being the RDS (Scheme 1).

We also observed a $^{1}H/^{2}H$ KIE of 0.953 (± 0.002) at the methylene bridge at "position d2" and a $^{1}H/^{2}H$ KIE of 0.965 (± 0.001) at "position d1". Since these two positions are not undergoing an sp^2 to sp^3 hybridization change, we did not initially expect an inverse KIE for these positions. We suspect that the inverse KIE at "positions d1 and d2" is due to some type of γ hyperconjugation effect.[44]

The conclusions of the KIE experiments were further validated by analyzing the reaction through DFT calculations using the ORCA 4.0.1 package (see Supporting Information for details). Our initial DFT calculations looked at the thermodynamics of pyridine dissociation from **G3-Di** to form **G3-Mono**, which served as an experimental benchmark for our calculations. A free energy of −2 kcal/mol was calculated when considering the effects of methylene chloride as a solvent using the conductor-like polarizable continuum model, CPCM. Although this moderate preference for **G3-Mono** in solution deviates slightly from the experimentally determined value of ΔG (+1 kcal/mol),[33] the solution phase enthalpy calculated using the electronic energy derived from the solvation free-energy calculation and the zero-point energy, is +12 kcal/mol. This value compares reasonably well with the experimentally determined ΔH of +10 kcal/mol. Furthermore, the ring opening of the three norbornenyl monomers were calculated to be exergonic, which is consistent with the release of the ring strain of the monomers.[45]

The transition state energies for the formation of the metallacyclobutane using norbornene, **M1-XX** and **M1-DD** (19.8, 19.7 and 22.3 kcal/mol, respectively), are the highest energies of the reaction profile, which is consistent with our experimental results that formation of the metallacyclobutane ring is the RDS. It is worth noting the higher transition state energies for the endo monomer (**M1-DD, TS1b**) over the exo monomer (**M1-XX, TS1c**). This difference is consistent with the experimental observation that the endo monomer polymerizes at a slower rate than the exo monomer. In contrast, the collapse of the metallacyclobutane ring is nearly barrierless. Such a low energy transition state is expected due to the strain present in the four-membered ring of the metallacyclobutane. This result was confirmed for norbornene and **M1-DD**, and even though we were unable to locate a TS for **M1-XX**, there is a consistent trend among the three profiles as can be seen in Figure 2. Besides validating our experimental evidence obtained through kinetic studies, the determination of the transition state energy via DFT enables us to rapidly probe whether the RDS of the reaction remains the same using other norbornene derivatives; this is important, as a change in the RDS leads to a change in the rate law for the polymerization.

Having determined the RDS, we derived the rate law for the polymerization of norbornenyl monomers initiated by **G3** (eq 1) ($K_{eq\,1}$ is shown in Scheme 2). This rate law predicts non-first-order behavior for [monomer], but experiments show that it is first order. This is explained by pyridine coordination being much stronger than the monomer coordination ($\frac{[Pyr]}{K_{eq1}[monomer]} \gg 1$) which makes the '+1' in the denominator insignificant. This simplified rate law is also consistent with previously reported data.[33]

Theoretical Rate Law with Step 2 as RDS:

$$\text{Rate} = \frac{k_2[\text{Ru}]_o}{\left(1 + \frac{[\text{Pyr}]}{K_{eq1}[\text{monomer}]}\right)} \approx \frac{k_2 K_{eq1}[\text{Ru}]_o[\text{monomer}]}{[\text{Pyr}]} \quad (1)$$

Exo-Endo Rate Study and Chelation Effects. Endo-substituted norbornenes are known to undergo ROMP significantly slower than their exo analogs. This difference in reactivity is presumably caused by a combination of the sterics/electronics of the monomer (referred to as monomer control) and the sterics/electronics of the growing polymer on the Ru center (referred to as polymer control). The origin of

DOI: 10.1021/jacs.9b09752
J. Am. Chem. Soc. 2019, 141, 17918−17925

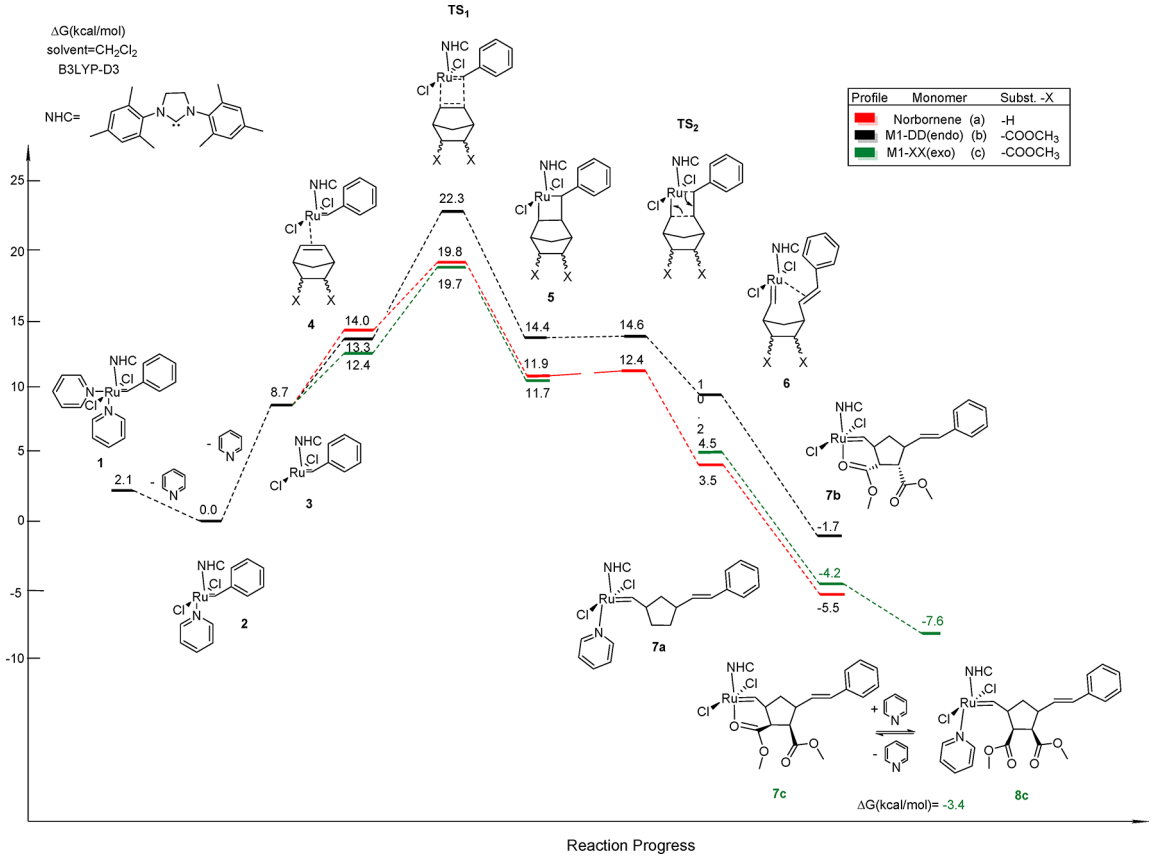

Figure 2. Free energy profile for the initiation of G3 with norbornene, **M1-DD**, and **M1-XX**.

Scheme 2. Thermodynamic Equilibria between Ester, Monomer, and Pyridine Coordination to the Ruthenium Center

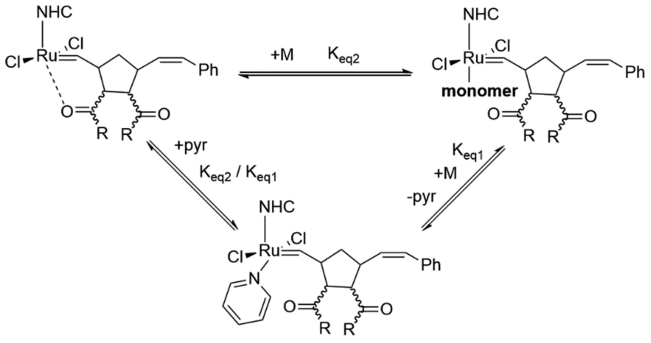

the exo/endo rate difference has been studied before with dicyclopentadiene, where kinetic evidence suggests that the steric encumbrance of the substituents in the endo monomer slows down the polymerization of this isomer (monomer control).[38,39]

For ester-containing monomers, it has been suggested that the ester from the proximal repeating unit can coordinate to the Ru center and slow down the polymerization ($K_{eq\ 2}$, Scheme 2). This ester coordination was postulated to be the main cause for the rate differences between **M2** and an **M1**-like monomer.[21] However, DFT calculations and kinetic measurements in the presence of chelate-opening agents did not validate this hypothesis for structurally similar monomers.[37] In another report, DFT calculations suggest that within one monomer set (**M1**) the endo polymer ester coordinates more

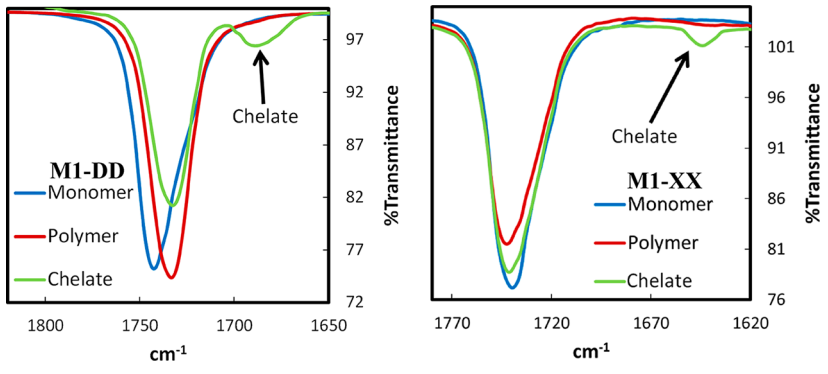

Figure 3. Overlaid IR spectrum for the monomer (blue), polymer (red), and chelate (green) for **M1-DD** (left) and **M1-XX** (right).

DOI: 10.1021/jacs.9b09752
J. Am. Chem. Soc. 2019, 141, 17918−17925

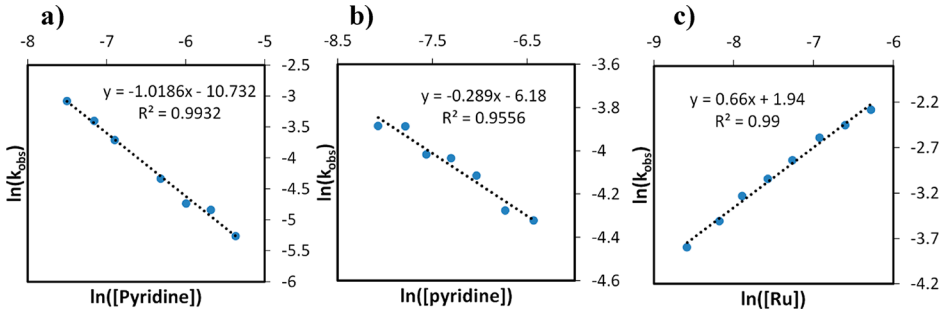

Figure 4. (a) **M2-DD** plot of ln (k_{obs}) versus ln([pyridine]). (b) **M1-DD** plot of ln(k_{obs}) versus ln([pyridine]) at constant Ru loading. (c) **M1-DD** plot of ln(k_{obs}) versus ln([Ru]) without added pyridine.

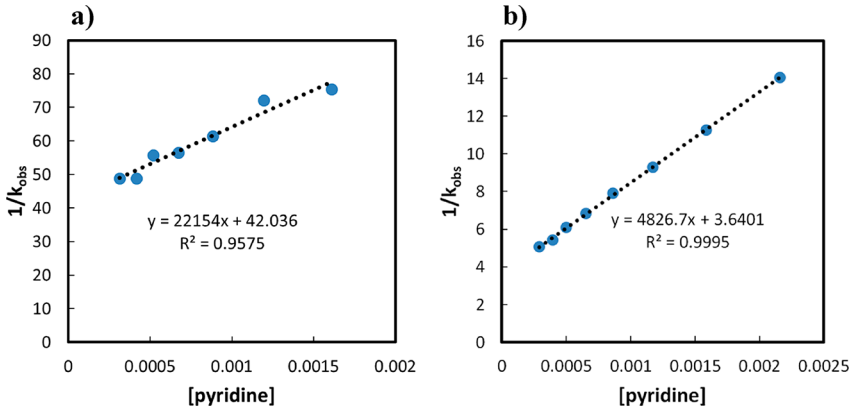

Figure 5. Plot of $1/k_{obs}$ versus [pyridine] for **M1-DD** (a) and for **M1-XX** (b).

strongly than the exo polymer ester and, thus, is responsible in part for the exo/endo rate difference.[5] We initiated an experimental kinetic and spectroscopic investigation to further understand whether ester coordination causes the exo/endo rate difference, and how ester coordination changes between monomer types.

We first investigated the formation of the chelate spectroscopically. In CH_2Cl_2 2 equiv of **M2-DD** was reacted with 1 equiv of **G3-Mono** at room temperature, and the crude mixture was analyzed by FTIR. No new carbonyl peak in the IR consistent with a chelated structure was observed with **M2-DD**. The same experiment with **M1-DD**, however, resulted in a new lower energy IR band at 1691 cm^{-1} compared to that of the polymer at 1691 cm^{-1}, which is consistent with the electron donation from the Ru into the chelated carbonyl weakening the bond (Figure 3).[46] This chelate was also observed for the other isomer **M1-XX**. The intensity of the lower energy carbonyl signals could be diminished upon addition of excess pyridine or completely suppressed upon addition of a stronger ligand (4-(dimethylamino)pyridine), which supports the conclusion that the new signal at 1733 cm^{-1} is the chelated complex (see Supporting Information Figure S5). While **M1** and **M2** are structurally very similar, only **M1** resulted in a coordinated ester; we postulate that the reason for this difference is due to the more stable ring size of the chelate for **M1** (six member for **M1** and eight member for **M2**). While no other chelating structures have been observed previously with **G2** or **G3** initiated polymerizations, these spectroscopic observations are consistent with a previous report using **G1** that observed a new alkylidene signal in the ^1H NMR consistent with a coordinated ester using an **M1** type monomer.[47,48]

Evidence supporting the chelate formation led us to reconsider the rate law for the polymerization, as ester coordination should compete with monomer (and pyridine) coordination and thus slow down the rate (Scheme 2). Taking that into consideration, we derived a new rate law under pre-equilibrium conditions (eq 2).

Theoretical Rate Law for Scheme 2 with k_2 as the RDS:

$$\text{Rate} = \frac{k_2[\text{Ru}]_o}{\left(1 + \frac{[\text{Pyr}]}{K_{eq1}[\text{monomer}]} + \frac{1}{K_{eq2}[\text{monomer}]}\right)} \approx \frac{k_2[\text{Ru}]_o[\text{monomer}]}{\left(\frac{[\text{Pyr}]}{K_{eq1}} + \frac{1}{K_{eq2}}\right)} \quad (2)$$

In eq 2, the ester coordination term is additive to that of pyridine coordination, meaning that if ester coordination is non-negligible the observed pyridine order of the reaction should be less than 1. **M2-DD** was determined experimentally to be inverse first order in pyridine (Figure 4a), suggesting that any ester coordination is negligible under pre-equilibrium conditions. This is consistent with the fact that no chelate was detected by IR spectroscopy for this monomer. For **M1-DD**, we measured that the polymerization is inverse 0.29 order in pyridine (Figure 4b) suggesting that ester chelation competes with monomer and pyridine for the coordination site which again is consistent with the chelate observed by IR spectroscopy.

In the absence of extra pyridine, the polymerization of **M1-DD** was measured to be 0.66 order in ruthenium (Figure 4c), which is consistent with **G3-Di** releasing 1 equiv of pyridine into solution and ester coordination. The polymerization

DOI: 10.1021/jacs.9b09752
J. Am. Chem. Soc. 2019, 141, 17918−17925

Scheme 3. Representation of How Ester Chelation Affects the Rate of Polymerization, But Not Catalyst Initiation

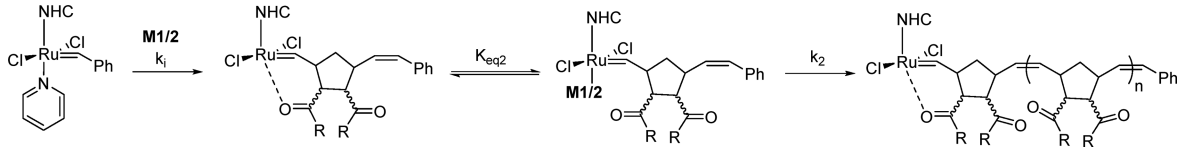

becomes first order in ruthenium when excess pyridine is added to the reaction mixture (see Supporting Information Figure S7). The relative binding strength of the chelating ester for a given monomer relative to pyridine can be determined by studying the rate of polymerization as a function of pyridine concentration. By rearranging eq 2 we obtain a linear relationship between $1/k_{obs}$ and [pyridine] (eq 3); the ratio between the slope and *y*-intercept of this linear equation corresponds to the relative binding strength (eq 4). For **M1-DD** we measured pyridine coordination to be 527 times stronger than ester coordination (Figure 5a), but because of the low concentration of pyridine in solution the majority of the catalyst shifts to the ester bound state. In comparison, for **M1-XX**, pyridine coordination was measured to be 1326 times stronger than ester coordination (Figure 5b). Overall this means that the endo polymer ester chelates ca. 2.5 times more strongly than the exo isomer, which establishes that ester coordination contributes to the differences in reactivity between the endo and exo isomers for **M1**.

Rearrangement of eq 2:

$$k_{obs} \approx \frac{k_2[\mathrm{Ru}]_o}{\left(\frac{[\mathrm{Pyr}]}{K_{eq1}} + \frac{1}{K_{eq2}}\right)}$$

$$\frac{1}{k_{obs}} \approx \frac{[\mathrm{Pyr}]}{K_{eq1}k_2[\mathrm{Ru}]_o} + \frac{1}{K_{eq2}k_2[\mathrm{Ru}]_o} \quad (3)$$

Relative Binding Strength of Pyridine and Chelate:

$$\frac{\mathrm{Slope}}{\mathrm{Intercept}} \approx \frac{K_{eq2}}{K_{eq1}} \quad (4)$$

We also probed the coordination of the ester via DFT and confirmed that the carbonyl oxygen from the proximal ester group from **M1-XX** forms a stable six membered chelate (Figure 2, Structure **7c**). Going from the ester complex to the pyridine complex, the ΔG was determined to be −3.4 kcal/mol from DFT, which is in good agreement with the experimentally determined value of −4.3 kcal/mol (based on 1326 equilibrium constant at 24.5 °C).

Having established that ester coordination contributes to the differences in rates of polymerization between the exo and endo monomers for **M1**, we went on to probe whether the incoming monomer (monomer control) contributes as well. The extent of monomer control can be determined experimentally by studying the difference in rate of initiation of **G3** with the pure exo and endo isomers, as initiation has no polymer control contribution (Scheme 3). By comparing the rates of polymerization for each pure monomer to the rate of initiation, we can determine to what extent polymer and monomer control contribute to the exo/endo rate difference.

As can be seen in Table 2, the rate of initiation using the **M2-XX** monomer is 4.7 times faster than that with **M2-DD**, which shows that the stereochemistry of the incoming monomer is a major contributor to the exo/endo rate difference. **M2-XX** was then measured to polymerize 5.2 times faster than **M2-DD**; the agreement between the initiation and polymerization values suggests that the differences in rate for polymerization between exo and endo for **M2** are primarily due to the incoming monomer (monomer control), which is consistent with the absence of chelate formation.

Table 2. Relative Rates of Initiation and Polymerization for ROMP of M1 and M2

Monomer	Initiation	Polymerization
M1-XX vs M1-DD	4.1	10.2
M2-XX vs M2-DD	4.7	5.2
M1-XX vs M2-XX	1.6	NA
M1-DD vs M2-DD	1.9	NA

M1-XX was determined to initiate 4.1 times faster than **M1-DD**, while it polymerizes 10.2 times faster. This is consistent with both monomer and polymer control contributing to the rate difference between exo and endo for **M1**, which again is consistent with the formation of an ester chelate. Comparing between monomer types we see that both **M1-XX** and **M1-DD** initiate faster than their **M2** counterparts, which suggests that the substituent groups coming off the norbornene also affect the reactivity of the monomer.

CONCLUSIONS

The rate-determining step for ROMP of a norbornene monomer using **G3** was determined to be formation of the metallacyclobutane ring using $^{12}C/^{13}C$ and $^{1}H/^{2}H$ kinetic isotope effect studies. This result was further validated by DFT calculations showing that the metallacyclobutane formation presented the higher transition state energy. The knowledge of the rate-determining step led to the derivation of a rate law describing the kinetics of ROMP of norbornene monomers. The origin of the exo/endo rate of polymerization was investigated through a series of kinetic experiments. The difference in rate appears to be primarily due to the stereochemistry of the incoming monomer for **M2**, while chelation (through ester coordination) and the incoming monomer contribute to **M1**. The ability of the **M1** polymer ester to coordinate to the Ru center is exemplified by the inverse 0.29 pyridine order in the rate law and the chelated species being observable in the IR. This in-depth mechanistic study provides the fundamental understanding needed to design next generation ROMP catalysts and monomers.

ASSOCIATED CONTENT

Supporting Information

The Supporting Information is available free of charge on the ACS Publications website at DOI: 10.1021/jacs.9b09752.

All experimental methods, materials and characterization (PDF)

DOI: 10.1021/jacs.9b09752
J. Am. Chem. Soc. 2019, 141, 17918−17925

AUTHOR INFORMATION

Corresponding Author

*guironne@illinois.edu

ORCID

Richard L. Lord: 0000-0001-6692-0369

Damien Guironnet: 0000-0002-0356-6697

Notes

The authors declare no competing financial interest.

ACKNOWLEDGMENTS

Umicore is acknowledged for the generous donation of metathesis catalyst. Major funding for the 500 MHz Bruker CryoProbe was provided by the Roy J. Carver Charitable Trust to the School of Chemical Sciences NMR Lab. This work was funded by NSF CHE 18-00068 and NSF DMR 17-27605.

REFERENCES

(1) Leitgeb, A.; Wappel, J.; Slugovc, C. The ROMP Toolbox Upgraded. *Polymer* **2010**, *51* (14), 2927−2946.

(2) Chen, Y.; Abdellatif, M. M.; Nomura, K. Olefin Metathesis Polymerization: Some Recent Developments in the Precise Polymerizations for Synthesis of Advanced Materials (by ROMP, ADMET). *Tetrahedron* **2018**, *74* (6), 619−643.

(3) Verduzco, R.; Li, X.; Pesek, S. L.; Stein, G. E. Structure, Function, Self-Assembly, and Applications of Bottlebrush Copolymers. *Chem. Soc. Rev.* **2015**, *44* (8), 2405−2420.

(4) Walsh, D. J.; Guironnet, D. Macromolecules with Programmable Shape, Size, and Chemistry. *Proc. Natl. Acad. Sci. U. S. A.* **2019**, *116* (5), 1538−1542.

(5) Chen, H.-Y.; Lee, B.; Chang, A. B.; Grubbs, R. H.; Lin, T.-P.; Liberman-Martin, A. L.; Luo, S.-X.; Thompson, N. B. Design, Synthesis, and Self-Assembly of Polymers with Tailored Graft Distributions. *J. Am. Chem. Soc.* **2017**, *139* (48), 17683−17693.

(6) Nowalk, J. A.; Fang, C.; Short, A. L.; Weiss, R. M.; Swisher, J. H.; Liu, P.; Meyer, T. Y. Sequence-Controlled Polymers Through Entropy-Driven Ring-Opening Metathesis Polymerization: Theory, Molecular Weight Control, and Monomer Design. *J. Am. Chem. Soc.* **2019**, *141* (14), 5741−5752.

(7) Elling, B. R.; Xia, Y. Living Alternating Ring-Opening Metathesis Polymerization Based on Single Monomer Additions. *J. Am. Chem. Soc.* **2015**, *137* (31), 9922−9926.

(8) Gutekunst, W. R.; Hawker, C. J. A General Approach to Sequence-Controlled Polymers Using Macrocyclic Ring Opening Metathesis Polymerization. *J. Am. Chem. Soc.* **2015**, *137* (25), 8038−8041.

(9) Bielawski, C. W.; Grubbs, R. H. Living Ring-Opening Metathesis Polymerization. *Prog. Polym. Sci.* **2007**, *32*, 1−29.

(10) Choi, T.-L.; Grubbs, R. H. Controlled Living Ring-Opening-Metathesis Polymerization by a Fast-Initiating Ruthenium Catalyst. *Angew. Chem., Int. Ed.* **2003**, *42* (15), 1743−1746.

(11) Fu, L.; Sui, X.; Crolais, A. E.; Gutekunst, W. R. Modular Approach to Degradable Acetal Polymers Using Cascade Enyne Metathesis Polymerization. *Angew. Chem., Int. Ed.* **2019**, DOI: 10.1002/anie.201909172.

(12) Elling, B. R.; Su, J. K.; Feist, J. D.; Xia, Y. Precise Placement of Single Monomer Units in Living Ring-Opening Metathesis Polymerization. *Chem.* **2019**, DOI: 10.1016/j.chempr.2019.07.017.

(13) Scholl, M.; Ding, S.; Lee, C. W.; Grubbs, R. H. Synthesis and Activity of a New Generation of Ruthenium-Based Olefin Metathesis Catalysts Coordinated with 1,3-Dimesityl-4,5-Dihydroimidazol-2-Ylidene Ligands. *Org. Lett.* **1999**, *1* (6), 953−956.

(14) Garber, S. B.; Kingsbury, J. S.; Gray, B. L.; Hoveyda, A. H. Efficient and Recyclable Monomeric and Dendritic Ru-Based Metathesis Catalysts. *J. Am. Chem. Soc.* **2000**, *122* (34), 8168−8179.

(15) Gessler, S.; Randl, S.; Blechert, S. Synthesis and Metathesis Reactions of a Phosphine-Free Dihydroimidazole Carbene Ruthenium Complex. *Tetrahedron Lett.* **2000**, *41* (51), 9973−9976.

(16) Sanford, M. S.; Love, J. A.; Grubbs, R. H. A Versatile Precursor for the Synthesis of New Ruthenium Olefin Metathesis Catalysts. *Organometallics* **2001**, *20* (12), 5314−5318.

(17) Hong, S. H.; Wenzel, A. G.; Salguero, T. T.; Day, M. W.; Grubbs, R. H. Decomposition of Ruthenium Olefin Metathesis Catalysts. *J. Am. Chem. Soc.* **2007**, *129* (25), 7961−7968.

(18) Vougioukalakis, G. C.; Grubbs, R. H. Ruthenium-Based Olefin Metathesis Catalysts Coordinated with Unsymmetrical N-Heterocyclic Carbene Ligands: Synthesis, Structure, and Catalytic Activity. *Chem. - Eur. J.* **2008**, *14* (25), 7545−7556.

(19) Slugovc, C.; Demel, S.; Stelzer, F. Ring Opening Metathesis Polymerisation in Donor Solvents. *Chem. Commun.* **2002**, *34* (21), 2572−2573.

(20) Yasir, M.; Liu, P.; Tennie, I. K.; Kilbinger, A. F. M. Catalytic Living Ring-Opening Metathesis Polymerization with Grubbs' Second- and Third-Generation Catalysts. *Nat. Chem.* **2019**, *11* (5), 488−494.

(21) Slugovc, C.; Demel, S.; Riegler, S.; Hobisch, J.; Stelzer, F. The Resting State Makes the Difference : The Influence of the Anchor Group in the ROMP of Norbornene Derivatives. *Macromol. Rapid Commun.* **2004**, *25*, 475−480.

(22) Dunbar, M.; Balof, S.; LaBeaud, L.; Yu, B.; Lowe, A.; Valente, E.; Schanz, H.-J. Improved Molecular Weight Control in Ring-Opening Metathesis Polymerization (ROMP) Reactions with Ru-Based Olefin Metathesis Catalysts Using N Donors and Acid: A Kinetic and Mechanistic Investigation. *Chem. - Eur. J.* **2009**, *15* (45), 12435−12446.

(23) Lin, T. P.; Chang, A. B.; Chen, H. Y.; Liberman-Martin, A. L.; Bates, C. M.; Voegtle, M. J.; Bauer, C. A.; Grubbs, R. H. Control of Grafting Density and Distribution in Graft Polymers by Living Ring-Opening Metathesis Copolymerization. *J. Am. Chem. Soc.* **2017**, *139* (10), 3896−3903.

(24) Fu, L.; Zhang, T.; Fu, G.; Gutekunst, W. R. Relay Conjugation of Living Metathesis Polymers. *J. Am. Chem. Soc.* **2018**, *140* (38), 12181−12188.

(25) Zachara, J.; Nascimento, D. L.; Gawin, A.; Gawin, R.; Gun, P. A. Integrating Activity with Accessibility in Olefin Metathesis: An Unprecedentedly Reactive Ruthenium-Indenylidene Catalyst. *J. Am. Chem. Soc.* **2019**, *141*, 10626−10631.

(26) Bailey, G. A.; Foscato, M.; Higman, C. S.; Day, C. S.; Jensen, V. R.; Fogg, D. E. Bimolecular Coupling as a Vector for Decomposition of Fast-Initiating Olefin Metathesis Catalysts. *J. Am. Chem. Soc.* **2018**, *140*, 6931−6944.

(27) Song, J.-A.; Park, B.; Kim, S.; Kang, C.; Lee, D.; Baik, M.-H.; Grubbs, R. H.; Choi, T.-L. Living Polymerization Caught in the Act: Direct Observation of an Arrested Intermediate in Metathesis Polymerization. *J. Am. Chem. Soc.* **2019**, *141* (25), 10039−10047.

(28) Trzaskowski, B.; Grela, K. Structural and Mechanistic Basis of the Fast Metathesis Initiation by a Six-Coordinated Ruthenium Catalyst. *Organometallics* **2013**, *32* (13), 3625−3630.

(29) Macnaughtan, M. L.; Gary, J. B.; Gerlach, D. L.; Johnson, M. J. A.; Kampf, J. W. Cross-Metathesis of Vinyl Halides. Scope and Limitations of Ruthenium-Based Catalysts. *Organometallics* **2009**, *28* (9), 2880−2887.

(30) Anderson, D. R.; Hickstein, D. D.; O'Leary, D. J.; Grubbs, R. H. Model Compounds of Ruthenium−Alkene Intermediates in Olefin Metathesis Reactions. *J. Am. Chem. Soc.* **2006**, *128* (26), 8386−8387.

(31) Sanford, M. S.; Love, J. A.; Grubbs, R. H. Mechanism and Activity of Ruthenium Olefin Metathesis Catalysts. *J. Am. Chem. Soc.* **2001**, *123*, 6543−6554.

(32) Love, J. A.; Morgan, J. P.; Trnka, T. M.; Grubbs, R. H. A Practical and Highly Active Ruthenium-Based Catalyst That Effects the Cross Metathesis of Acrylonitrile. *Angew. Chem., Int. Ed.* **2002**, *41* (21), 4035−4037.

(33) Walsh, D. J.; Lau, S. H.; Hyatt, M. G.; Guironnet, D. Kinetic Study of Living Ring-Opening Metathesis Polymerization with Third-

DOI: 10.1021/jacs.9b09752
J. Am. Chem. Soc. 2019, 141, 17918−17925

Generation Grubbs Catalysts. *J. Am. Chem. Soc.* **2017**, *139* (39), 13644−13647.
(34) Hlil, A. R.; Balogh, J.; Moncho, S.; Su, H.-L.; Tuba, R.; Brothers, E. N.; Al-Hashimi, M.; Bazzi, H. S. Ring Opening Metathesis Polymerization (ROMP) of Five- to Eight-Membered Cyclic Olefins: Computational, Thermodynamic, and Experimental Approach. *J. Polym. Sci., Part A: Polym. Chem.* **2017**, *55* (18), 3137−3145.
(35) Neary, W. J.; Kennemur, J. G. Polypentenamer Renaissance: Challenges and Opportunities. *ACS Macro Lett.* **2019**, *8* (1), 46−56.
(36) Neary, W. J.; Isais, T. A.; Kennemur, J. G. Depolymerization of Bottlebrush Polypentenamers and Their Macromolecular Metamorphosis. *J. Am. Chem. Soc.* **2019**, *141*, 14220−14229.
(37) Radzinski, S. C.; Foster, J. C.; Chapleski, R. C.; Troya, D.; Matson, J. B. Bottlebrush Polymer Synthesis by Ring-Opening Metathesis Polymerization: The Significance of the Anchor Group. *J. Am. Chem. Soc.* **2016**, *138* (22), 6998−7004.
(38) Rule, J. D.; Moore, J. S. ROMP Reactivity of endo - and exo -Dicyclopentadiene. *Macromolecules* **2002**, *35* (21), 7878−7882.
(39) Robertson, I. D.; Pruitt, E. L.; Moore, S. Frontal Ring-Opening Metathesis Polymerization of Exo- Dicyclopentadiene for Low Catalyst Loadings. *ACS Macro Lett.* **2016**, *5*, 593−596.
(40) Moatsou, D.; Hansell, C. F.; O'Reilly, R. K. Precision Polymers: A Kinetic Approach for Functional Poly(Norbornenes). *Chem. Sci.* **2014**, *5* (6), 2246−2250.
(41) Romero, P. E.; Piers, W. E. Direct Observation of a 14-Electron Ruthenacyclobutane Relevant to Olefin Metathesis. *J. Am. Chem. Soc.* **2005**, *127*, 5032−5033.
(42) Sanford, M. *Synthetic and Mechanistic Investigations of Ruthenium Olefin Metathesis Catalysts*; California Institute of Technology: Pasadena, CA, 2001.
(43) Singleton, D. A.; Thomas, A. A. High-Precision Simultaneous Determination of Multiple Small Kinetic Isotope Effects at Natural Abundance. *J. Am. Chem. Soc.* **1995**, *117*, 9357−9358.
(44) Leffek, K. T.; Llewellyn, J. A.; Robertson, R. E. Some Deuterium Isotope Effects. III. An Inverse Gamma-Deuterium Isotope Effect. *J. Am. Chem. Soc.* **1960**, *82*, 6315−6318.
(45) Lebedev, B.; Smirnova, Y.; Makovetsky, K. Thermodynamics of Norbornene, of Its Polymerization Process and of Polynorbornene from 0 to 400 K at Standard Pressure. *Makromol. Chem.* **1992**, *193*, 1399−1411.
(46) Bryant, B.; Pariaud, J.-C.; Fernelius, C. The Infrared Spectra of Chelate Compounds I. A Study of the Carbonyl Frequencies of the Hydrogen and Metal Chelates of the Substituted Cycloheptatrienones. *J. Org. Chem.* **1954**, *19*, 1889−1896.
(47) Haigh, D. M.; Kenwright, A. M.; Khosravi, E. Nature of the Propagating Species in Ring-Opening Metathesis Polymerizations of Oxygen-Containing Monomers Using Well-Defined Ruthenium Initiators. *Macromolecules* **2005**, *38*, 7571−7579.
(48) We investigated the chelate formation with **G3** via variable temperature ^{1}H NMR; however, this study remains inconclusive due to the number of species present in solution and the dynamic exchange between some of these species (pyridine complex, dipyridine complex, and chelated complex). Additionally the low temperature disfavors chelation formation as the reaction is entropy driven.

DOI: 10.1021/jacs.9b09752
J. Am. Chem. Soc. 2019, 141, 17918−17925